SMASH HCM

DELIVERABLE

Project Acronym: **SMASH-HCM**

Grant Agreement number: **101137115**

Project Title: **Stratification, Management, and Guidance of Hypertrophic Cardiomyopathy Patients using Hybrid Digital Twin Solutions**

D4.1 – Libraries of HCM populations of cellular electromechanical models

Revision: 1.0

Authors and Contributors	Chiara Bartolucci (UNIBO); Alfonso Bueno-Orovio (OXF); Alan Fabbri (UNIBO); Jari Hyttinen (TAU); Jussi Koivumäki (TAU); Ossi Noita (TAU); Eugenio Ricci (UNIBO); Stefano Severi (UNIBO); Olli Ylinen (TAU)			
Responsible Author	Jussi Koivumäki		Email	jussi.koivumaki@tuni.fi
	Beneficiary	TAU	Phone	+358505056897

Project co-funded by the European Commission within HORIZON-HLTH-2023-TOOL-05-03		
Dissemination Level		
PU	Public, fully open	X
CO	Confidential, restricted under conditions set out in Model Grant Agreement	
CI	Classified, information as referred to in Commission Decision 2001/844/EC	

Funded by the European Union. Views and opinions expressed are however those of the author(s) only and do not necessarily reflect those of the European Union. Neither the European Union nor the granting authority can be held responsible for them.

Funded by the European Union

Revision History, Status, Abstract, Keywords, Statement of Originality

Revision History

Revision	Date	Author	Organisation	Description
0.1	19.05.	JK	TAU	Draft of the report structure and planned content.
0.2	26.05	JK	TAU	Added content on the POMs principle as well as previous work on mutations and the TAU work on JPH2 mutation.
0.3	07.06.	all	TAU, UNIBO	Contents ready for “WP internal” review.
0.4	11.06	JK	TAU	Revised version based on “WP internal” review. Version ready for “Consortium internal” review.
0.5	19.06.	JK	TAU, UNIBO	Revised version based on the “Consortium internal” review.
1.0	24.06.	JK	TAU	Final version.

Date of delivery	Contractual:	30.06.2025	Actual:	25.06.2025
Status	final ☒ /draft ☐			

Abstract (for dissemination)	This document presents deliverable ***D4.1 – Libraries of HCM populations of cellular electromechanical models*** of the SMASH-HCM project. We work entails 1) an open-source software tool for building populations of virtual heart cells, 2) a library of five mutation-specific model variants hypertrophic cardiomyopathy (HCM), and 3) the corresponding populations of healthy and mutated model variants. The established modelling and simulation framework will be employed in the work ahead, to stratify disease markers of electrophysiological and biomechanical abnormalities, and to predict safety and efficacy of candidate drug molecules, across HCM variants.
Keywords	computer modelling and simulations; cardiomyocytes; parameterisation; virtual populations

Statement of originality

This deliverable contains original unpublished work except where clearly indicated otherwise. Acknowledgement of previously published material and of the work of others has been made through appropriate citation, quotation, or both.

Table of Contents

List of Figures

Executive Summary

This deliverable **D4.1 – Libraries of HCM populations of cellular electromechanical models** ties in with the aims of task **T4.1 Precision cellular deep phenotyping for stratification in HCM** in WP4 of the SMASH-HCM project plan:

> ***T4.1 Precision cellular deep phenotyping for stratification in HCM*** *(M1-M36) (TAU-lead, UNIBO). We will integrate the effects of HCM mutations based on the domain knowledge and our clinical and in-vitro data. Phenotypic variability in the broader population will be investigated by exploiting a POMs approach to serve as in silico stratification tools for characterizing adverse phenotypes emerging from each specific genotype. POMs-derived features of cellular pro-arrhythmic factors will serve as additional data for WP6.*

Highlights:

- We have developed a scalable and user-friendly open-source software tool to specify and execute the simulations for building the so-called population of models (POMs) or databases of virtual cells.
- We have established a library of five HCM-related mutation-specific model variants that replicate the key functional alterations measured experiments.
- We have extended the model library of mutation variants to POMs, including the previously published work and two newly implemented HCM mutations.

The established modelling frameworks and implemented software tools will be expanded and exploited in the work ahead, to stratify disease markers of electrophysiological and biomechanical dysfunction, and to predict safety and efficacy of candidate drug molecules, across HCM variants.

1 Populations of models (POMs)

In this chapter, we briefly describe the basic idea of building a database of virtual heart muscle cells (cardiomyocytes, CMs), so-called *in silico* population of models (POMs), citing foundational publications for this approach, including our own relevant previously published studies.

1.1 Short description of the POMs approach

The approach of building virtual databases of cardiomyocytes, or *in silico* populations of models (POMs) was first introduced by Prinz *et al.* (2003) in the context of neuronal electrophysiology[1], and later popularised for the cardiomyocyte electrophysiology by Britton *et al.* (2013)[2]. For detailed of the methodology, we refer the reader to the review by Muszkiewicz *et al.* (2016)[3]. The process of constructing POMs is illustrated in Figure 1.

Figure 1 – POMs process

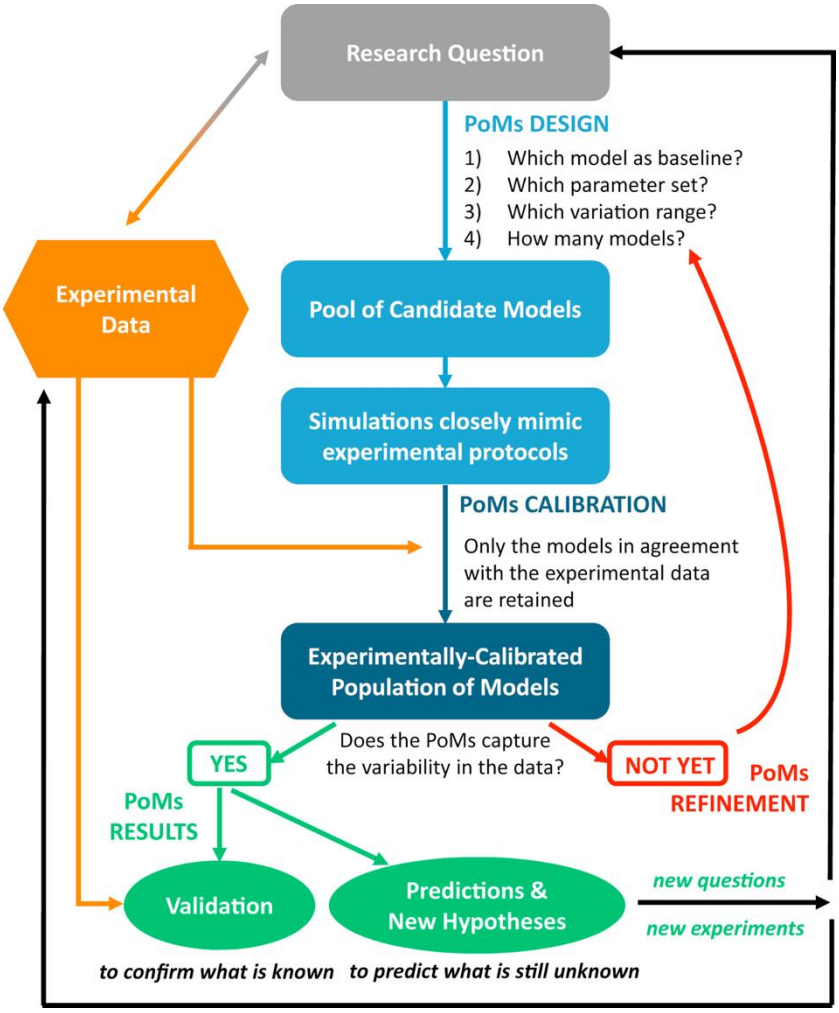

Flowchart of the process for constructing POMs (reproduced under Open Access licence from[3]).

[1] Prinz et al. (2003). Alternative to Hand-Tuning Conductance-Based Models: Construction and Analysis of Databases of Model Neurons. J.Neurophysiol. 90, 3998–4015. doi: 10.1152/jn.00641.2003

[2] Britton et al. (2013). Experimentally calibrated population of models predicts and explains intersubject variability in cardiac cellular electrophysiology. PNAS 110, E2098–E2105. doi: 10.1073/pnas.1304382110

[3] Muszkiewicz et al. (2016). Variability in cardiac electrophysiology: Using experimentally-calibrated populations of models to move beyond the single virtual physiological human paradigm. PBMB120, 115–27. doi: 10.1016/j.pbiomolbio.2015.12.002

Nowadays, POMs is an established **approach to addressing biological variability** observed in experimental data (ion channel conductances, cellular ion transporters, cell size/structure, etc.), and exploring biological robustness. Thus, it offers advantages in development of more accurately parameterised models and the testing of diagnostic or therapeutic strategies. For example, in vitro human induced pluripotent stem cell (hiPSC)-derived cardiomyocytes (hiPSC-CMs) tend to exhibit very high inter-cell, -batch, -subject, and -lab variability in their phenotype. Thus, using POMs is an excellent strategy to tackle, or to make sense of that variability. The basic concept of capturing biological variability with POMs is depicted in Figure 2.

A rather standard approach for **parameter randomisation to obtain a population** of some thousands of virtual CMs is by:

- selecting a subset of 15-20 parameters from the model to be varied,
- varying the parameter values in the range of [50–200] % (or multiplied by [0.5, 2]) from the baseline value, and
- using an appropriate sampling technique, such as Latin Hypercube Sampling (LHS), to generate an initial distribution of plausible combinations of model parameter values from the multidimensional distribution.

We have used this approach in our work; specific details are available in Chapter 2.2.

Next step in the POMs process is to run simulations with the whole generated population of candidate models. To obtain a so-called **experimentally-calibrated population**, the candidate model's outputs are compared to electro-chemo-mechanical biomarkers calculated from *in vitro* data. The acceptable model outputs fall within the experimentally observed ranges of biomarkers. Calibration criteria vary, depending on the available data, which is illustrated in Figure 2. Smaller datasets rely on expert judgment, while larger ones allow statistical methods like standard deviation thresholds. Recent approaches explore combining multiple data types and using flexible calibration bounds or likelihood estimators to better reflect physiological variability and improve predictive power, especially when large datasets are available.

Figure 2 – POMs and variability of data

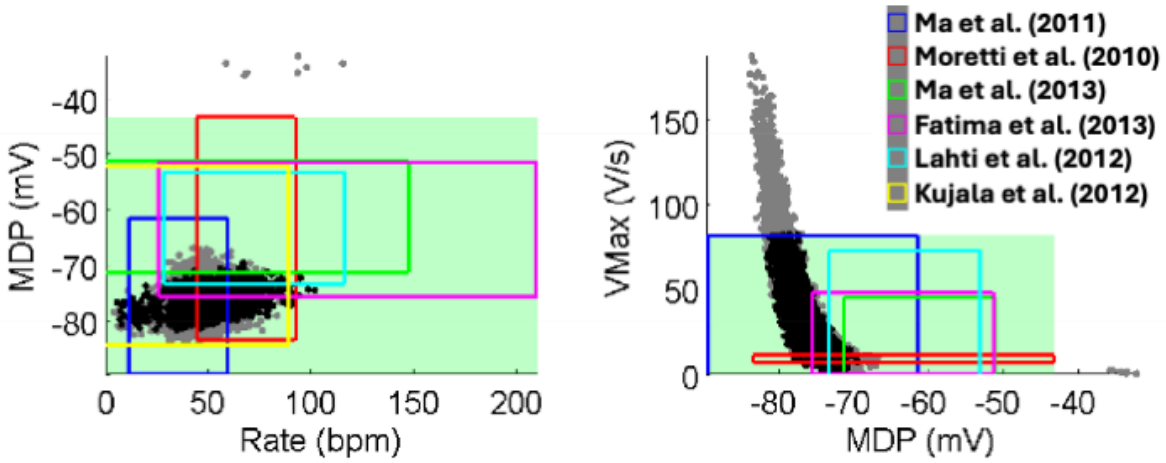

Illustration of how virtual population is calibrated with experimental data set to replicate biological variability. Scatter plots show biomarker values for accepted = black dots and rejected = grey dots hiPSC-CM models in the in silico database. MDP = Minimum diastolic potential, Rate = spontaneous beating rate, and Vmax = Maximum velocity of the upstroke phase of the action potential (Figure reproduced under Open Access licence from[4].)

[4] Paci et al. (2017). Phenotypic variability in LQT3 human induced pluripotent stem cell-derived cardiomyocytes and their response to antiarrhythmic pharmacologic therapy: An in silico approach. Heart Rhythm 14, 1704–1712. doi: 10.1016/j.hrthm.2017.07.026

1.2 Alternative ways of obtaining diseased/mutated subpopulations

The three principal routes for obtaining POMs from the baseline model are shown in the schematic below (Figure 3).

Figure 3 – How to obtain healthy and diseased subpopulations?

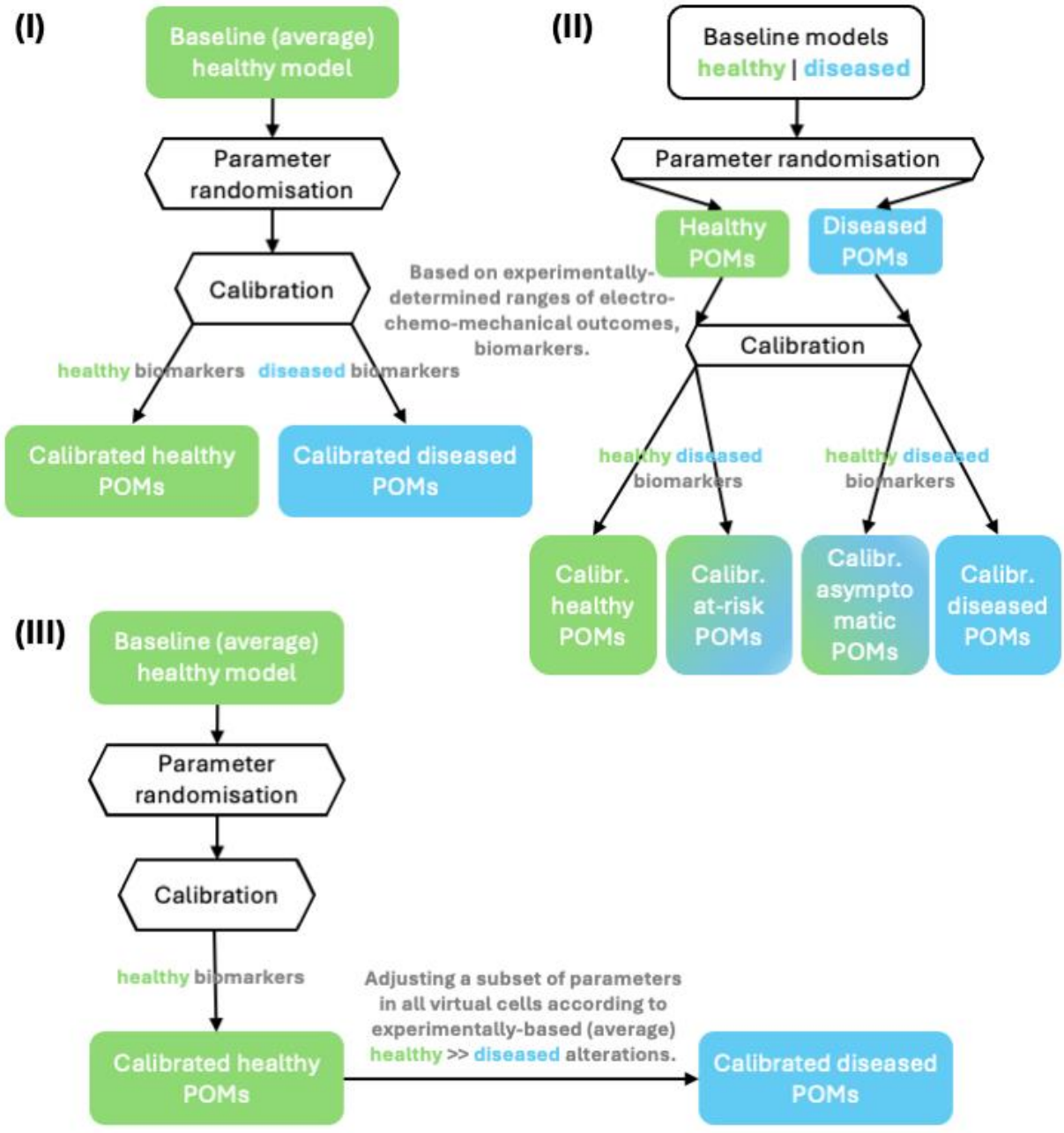

Please refer to chapter 1.1 for definition of the terms "calibration" and "parameter randomisation". Approach I is the most straightforward and commonly used one, as it does not require data on the disease mechanism. Approach II takes advantage of the known (or speculated) disease mechanisms, and it can be employed to investigate the overlap or diffusion of healthy and diseased POMs. Approach III is beneficial, when quantified understanding of the disease mechanisms does exist, while there is limited in vitro data characterising the disease phenotype.

2 POMs software and workflow

In this chapter, we describe the tools newly implemented in SMASH-HCM WP4 for POMs and the pipeline for using them, as well as the workflow related to the existing tools developed previously by our consortium partners.

For the SMASH-HCM internal use, we have also established an internal repository (in our MS Teams group) for sharing the CM model source codes, characterisations and model implementations of disease variants, as well as POMS-related parameter lists, biomarker tables, analysis scripts, etc.

2.1 Description of the implemented open-source POMs tool

The new tool provides an easy and reproducible way to generate large population of models. To achieve translation from in-house custom research software to freely available open-source standard software, new software was built with/for:

- broader functionality, covering a wide range of use cases;
- compatibility with different computing platforms, e.g. Matlab, OpenCarp, etc.;
- better scalability and support for cluster-based computing;
- user-friendly design, emphasising intuitive interface/operation;
- proper documentation.

The calculation of biomarkers has commonly been done either with proprietary software or with custom in-house tools. This makes sharing work complex, as there might be different conventions. The tool is command line interface based on python that can be divided into three distinct steps. Its basic functionality is to run a user defined model, calculate biomarkers, and calibrate a population (Figure 4).

To use the tool, the user only needs to be able to run their *in silico* model from the command line. This means the tool can be used with platforms such as Matlab, OpenCarp, myokit, without changes to existing code. The user needs to define configurations for the experiment, which detail how the *in silico* model is used and what kind of population they want to create. Config files are easy to share, so other teams can use those to reproduce results, supporting the FAIR (Findable, Accessible, Interoperable and Reusable) principles. Or, similarly, to create new populations using the same settings.

The number of runs needed to create a population can be large, with population sizes often in the order of 10,000 models, and each single model run potentially taking minutes. That is why the tool allows to execute runs in patches, making parallelisation of the tasks possible. Patches can be combined to make the results the same as it would have been without running it in patches.

The POM tool will be made publicly available with permissive licence. Open source allows people to trust the results and expand the tool for their purposes. In this way, the tool can be used by other researchers, and new features can be developed and suggested by the wider research community. With opening our tools to the wider community, further feedback to the documentation can be made available, leading to better final documentation than normal custom tools.

The tool is currently available at https://github.com/TAU-CBIG/POMtool.

Figure 4 – POM tool workflow

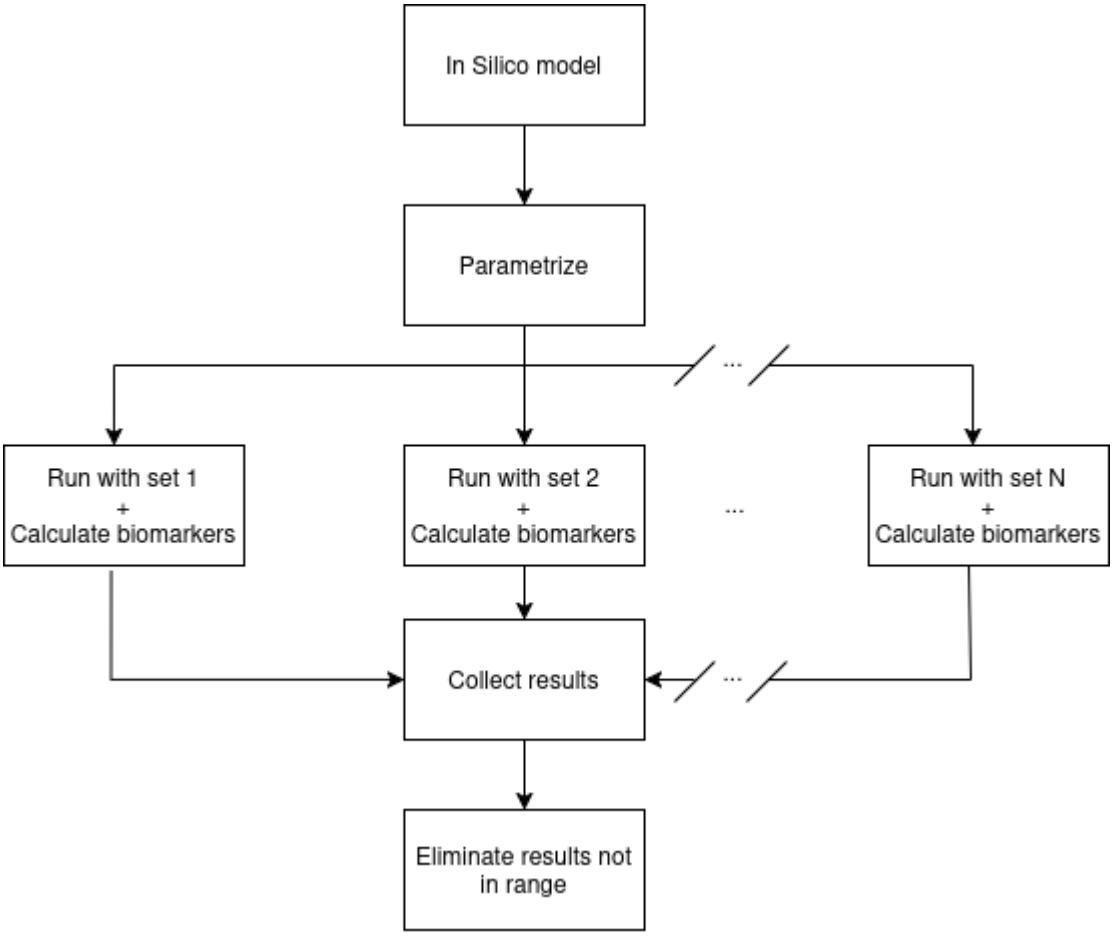

POM Tool start with user defined way to run the model. This model is then parametrized. After this, model is run with each define parameter set and biomarkers are calculated. Then results are collected, and the model variants producing results that do not match the given biomarker ranges can be eliminated.

2.2 Recipe for running POMs simulations with the new tool

As described in Figure 4, the population building starts by selecting the subset of parameters that will be randomly varied in the baseline CM model. For our purposes, we selected the parameters listed below separately for the hiPSC-CM and native human ventricular myocyte (hv-CM) models in Table 1.

Table 1 – Model parameter subset used for POMs

	hiPSC-CM	**hv-CM**	**Parameter explanation**
Electrophysiology	gNa	GNa	Maximal conductance of the fast sodium-current
	gNaL	GNaL	Maximal conductance of the late sodium current
	gK1	GK1	Maximal conductance of the inward rectifier current
	gKr	GKr	Maximal conductance of the rapid delayed rectifier current
	gKs	GKs	Maximal conductance of the slow delayed rectifier current

	gKto	Gto	Maximal conductance of the transient outward current
	gNKA	Gnak	Maximal conductance of the sodium-potassium pump
Calcium cycling	gNCX	Gncx	Maximal conductance of the sodium-calcium exchanger
	Jrel_max	Jrel_max	Maximal flux of release from sarcoplasmic reticulum
	Jup_max	Jup_max	Maximal flux uptake by sarcoplasmic reticulum
	gCaL	PCaL	Maximal conductance of the L-type calcium current
	tau_f1	Tau_f	fast time constant of voltage-dependent ICaL inactivation
	tau_f2	Tau_s	slow time constant of voltage-dependent ICaL inactivation
	tau_fCa	Tau_Ca	Time constant of Ca^{2+}-dependent ICaL inactivation
Contractility	Pi_ref (mM)	nperm	Reference value for inorganic phosphate; Exponent of the Hill equation for Ca-Troponin/unblocked myosin binding sites
	MgADP (mM)	ca50	Magnesium-adenosine diphosphate concentration; Half-activation value of Ca^{2+} binding to troponin
	ap2 coef	Ktm unblock	Crossbridge detachment coefficient; Transition rate from blocked to unblocked state of myosin heads
	F1	Kws	Coefficient affecting pre-rotational states in crossbridge cycling; Transition rate from weakly to strongly bound myosin heads
	F2	Kuw	Coefficient affecting pre-rotational states in crossbridge cycling; Transition rate from unblocked to weakly bound myosin heads

An initial population of 10,000 cells was obtained by randomising the 19 parameters in Table 1 using the Latin Hypercube Sampling method in the [50%, 200%] range for both hiPSC-CM and hv-CM models.

Then, simulations were run for 200 paced beats at a cycle length (CL) of 1000 ms with each randomized parameter set to obtain action potential (AP), calcium transient (CT) and active tension (AT) traces, on which biomarkers could be computed. Calibration of the *in silico* populations consisted in discarding those parameters combinations that yielded biomarkers outside of experimental ranges reported from literature or experiments. In the case of hv-CM, Table 2 reports the biomarkers considered for the pruning and the adopted [minimum, maximum] intervals.

Table 2 – Biomarkers data for experimental calibration of the hv-CM model

	Biomarker	Unit of measure	Min	Max

Action potential	APD_{40}	ms	85	320
	APD_{50}	ms	110	350
	APD_{90}	ms	188	440
	Tri_{90-40}	ms	50	150
	dV/dt_{max}	mV/ms	100	1000
	V_{peak}	mV	10	55
	RMP	mV	-95	-80
Calcium transient	CTD_{50}	ms	120	420
	CTD_{90}	ms	220	785
	CT_{peak}	mM	0.000262	0.00223
	CT_{diast}	mM	0	0.0004
Active tension	TTP	ms	147	172
	RT_{50}	ms	109	125
	RT_{95}	ms	291	377
	At_{peak}	kPa	15	25
	AT_{min}	kPa	0	-

APD40-50-90, AP duration at 40, 50, 90 % of repolarisation; Tri, AP triangulation index; dV/dtmax, maximum upstroke velocity; Vpeak, maximum membrane potential; RMP, resting membrane potential; CT50 and CT90, calcium transient duration at 50 and 90 % of decay; CTpeak and CTdiast, calcium transient peak and diastolic concentrations; TTP, time to peak tension; RT50 and RT90, time from peak contraction to 50 and 90 % of relaxation; ATpeak and ATmin, max and min values of active tension. Min and Max experimental ranges from [5,6].

Due to the very restrictive experimental ranges for active tension biomarkers, the same approach of [5,6,7] was adopted: a cost function measuring the distance between the computed biomarker and its ranges was implemented. In this way, cells that showed a total distance below a specific threshold were accepted during calibration. For the hv-CM BPS model, a threshold value of 100 was necessary to obtain a sufficient number of calibrated cells in the population, while still maintaining AT biomarkers close to the experimental ranges.

To obtain the mutant populations, the parameter modifications obtained from the single cell modelling below (Section 3.2) were applied to the calibrated control cell population. Cells that following the mutation showed: 1) unphysiological ion concentrations (intracellular sodium between 5 and 15 mM, diastolic calcium lower than 150 nM, systolic calcium above 200 nM, and sarcoplasmic reticulum calcium between 0 and 10 mM), 2) repolarisation failure, or 3) early afterdepolarisations, were automatically discarded from subsequent analysis (but kept for population statistics).

[5] Margara et al. (2022). Mechanism based therapies enable personalised treatment of hypertrophic cardiomyopathy. Sci Rep. 12(1):22501. doi: 10.1038/s41598-022-26889-2.

[6] Mora et al. (2023). Insights from an electro-mechanical heart failure cell model: Role of SERCA enhancement on arrhythmogenesis and myocyte contraction. Comput Methods Programs Biomed. 230:107350. doi: 10.1016/j.cmpb.2023.107350.

[7] Land et al. (2017). A model of cardiac contraction based on novel measurements of tension development in human cardiomyocytes. J Mol Cell Cardiol. 106:68-83. doi: 10.1016/j.yjmcc.2017.03.008.

Once the populations were obtained, 3 different protocols of afterdepolarizations induction were performed, as in [8]:

- Fast pacing (1500 beats at CL = 275 ms) followed by a 10 s pause to elicit delayed afterdepolarizations (DADs).
- Slow pacing (20 beats at CL = 4000 ms) plus 20 µM quinidine administration, simulated by blocking I_{Na}, I_{Kr}, I_{CaL}, I_{Ks} and I_{to} maximal conductances by 59.5%, 98.3%, 86.4%, 87.8% and 90.6%, respectively, according to their IC_{50} values.
- Slow pacing (20 beats at CL = 5000 ms) plus 0.1 µM dofetilide administration, simulated by blocking I_{Kr} maximal conductance by 93.8% with altered ionic concentrations ($[K^+]_o$ = 5 mM, $[Ca^{2+}]_o$ = 2 mM and $[Na^+]_o$ = 137 mM).

A logistic regression approach[9] was adopted to investigate the role of model parameters in influencing early afterdepolarisation (EADs) inducibility, while linear regression[10] was performed to gain insights on the role of the parameters in determining the output biomarkers.

2.3 The selected baseline in silico cardiomyocyte models

Cardiomyocyte models described in Table 3 were selected for building the celltype-specific populations of models.

Table 3 – Cardiomyocyte models

Celltype	Identificator	Notes	Ref
hiPSC-CM	hiPSC-CM	Includes the Tran *et al.* contractile element module.	**11**
hv-CM	ORd+Land	Includes the Land *et al.* contractile element module.	**12**
	ToRORd+Land	Includes the Land *et al.* contractile element module.	**12**
	BPS+Land	Includes the Land *et al.* contractile element module.	**8**

[8] Bartolucci et al. (2022). A Novel *In Silico* Electromechanical Model of Human Ventricular Cardiomyocyte. Front Physiol. 13:906146. doi: 10.3389/fphys.2022.906146.

[9] Morotti et al. (2016). Logistic regression analysis of populations of electrophysiological models to assess proarrythmic risk. MethodsX 4:25-34. doi: 10.1016/j.mex.2016.12.002.

[10] Morotti et al. (2017). Predominant contribution of L-type Cav1.2 channel stimulation to impaired intracellular calcium and cerebral artery vasoconstriction in diabetic hyperglycemia. Channels (Austin). 11(4):340-346. doi: 10.1080/19336950.2017.1293220.

[11] Forouzandehmehr et al. (2024). In silico study of the mechanisms of hypoxia and contractile dysfunction during ischemia and reperfusion of hiPSC cardiomyocytes. Dis Model Mech 17, dmm050365. doi: 10.1242/dmm.050365

[12] Margara et al. (2021). In-silico human electro-mechanical ventricular modelling and simulation for drug-induced pro-arrhythmia and inotropic risk assessment. PBMB 159, 58–74. doi: 10.1016/j.pbiomolbio.2020.06.007

3 Results

In this chapter, we present the computational modelling and simulation results, employing implementation of five hiPSC-CM and hv-CMs model variant that recapitulate the *in vitro* characterisation of HCM phenotypes (i.e., altered function caused by HCM-related mutations).

Summary of HCM mutations (-> encoded protein) selected as SMASH-HCM targets for in vitro classification, in silico simulations, and also clinical materials:

- MYH7 (R403Q) -> the beta myosin heavy chain of thick filament (sarcomeric),
- TNNT2 (R92Q) -> the cardiac troponin T protein (sarcomeric),
- TNNI3 (R21C) -> the cardiac isoform, I3, of troponin I3 protein (sarcomeric),
- MYBPC3 (c.772G>A) -> the cardiac isoform of myosin-binding protein C (sarcomeric),
- JPH2 (T161K) -> the cardiac isoform, JPH2, of junctophilin protein (non-sarcomeric).

3.1 Brief description of the previously published work

3.1.1 MYH7 (R403Q), TNNT2 (R92Q), and TNNI3 (R21C) in hv-CMs

Figure 5 and Figure 6 illustrate how the mutated phenotypes were replicated *in silico* based on *in vitro* data from hv-CMs in the previous work by OXF[Error! Bookmark not defined.].

Figure 5 – Mechanistic characterisation of the MYH7(R403Q) cellular phenotype in hv-CM

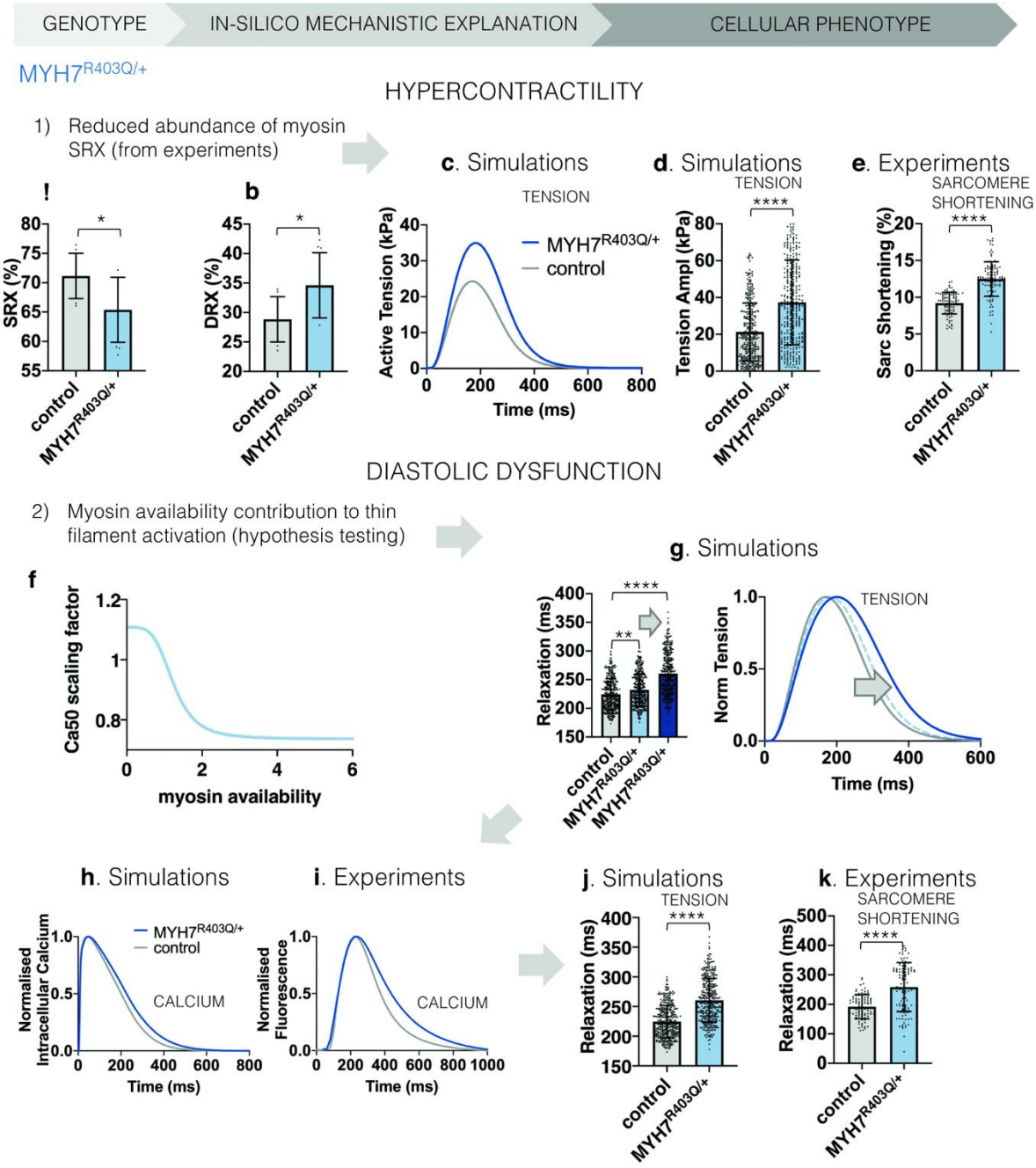

Human-based modelling and simulation replicates the biophysical findings of hypercontractility and diastolic dysfunction through shown in vitro. (Figure reproduced under Open Access licence from [Error! Bookmark not defined.]*).*

Figure 6 – Mechanistic characterisation of the TNNT(2R92Q) and TNNI3(R21C) cellular phenotypes in hv-CM

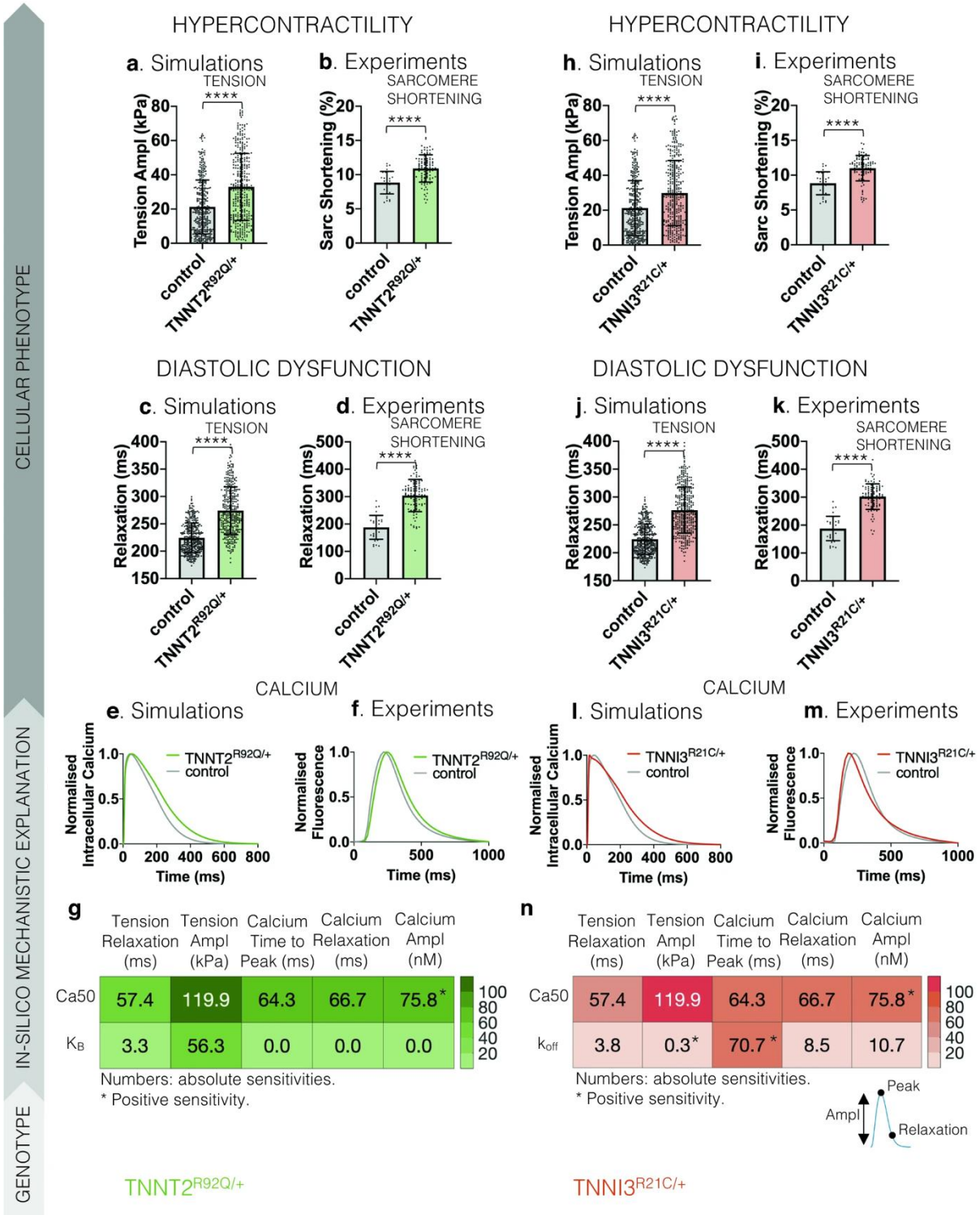

Human-based modelling and simulation replicates the biophysical findings of hypercontractility and diastolic dysfunction through shown in vitro. (Figure reproduced under Open Access licence from[Error! Bookmark not defined.]).

3.1.2 MYH7 (R403Q) in hiPSC-CMs

Figure 7 shows that incorporating energetics in the contractile element (CE) of hiPSC-CM model (referred to as hiMCE in the Figure) captures accurately the HCM-related changes ~33% prolongation of relaxation in active tension (panel C) and ~40% increase in fractional cell shortening due to the

R403Q mutation (panel F), matches experimental findings. The biomarkers characterising the disease phenotype are summarised in Table 4. This is previously published work from TAU[13].

Figure 7 – Mechanistic characterisation of the MYH7(R403Q) cellular phenotype in hiPSC-CM

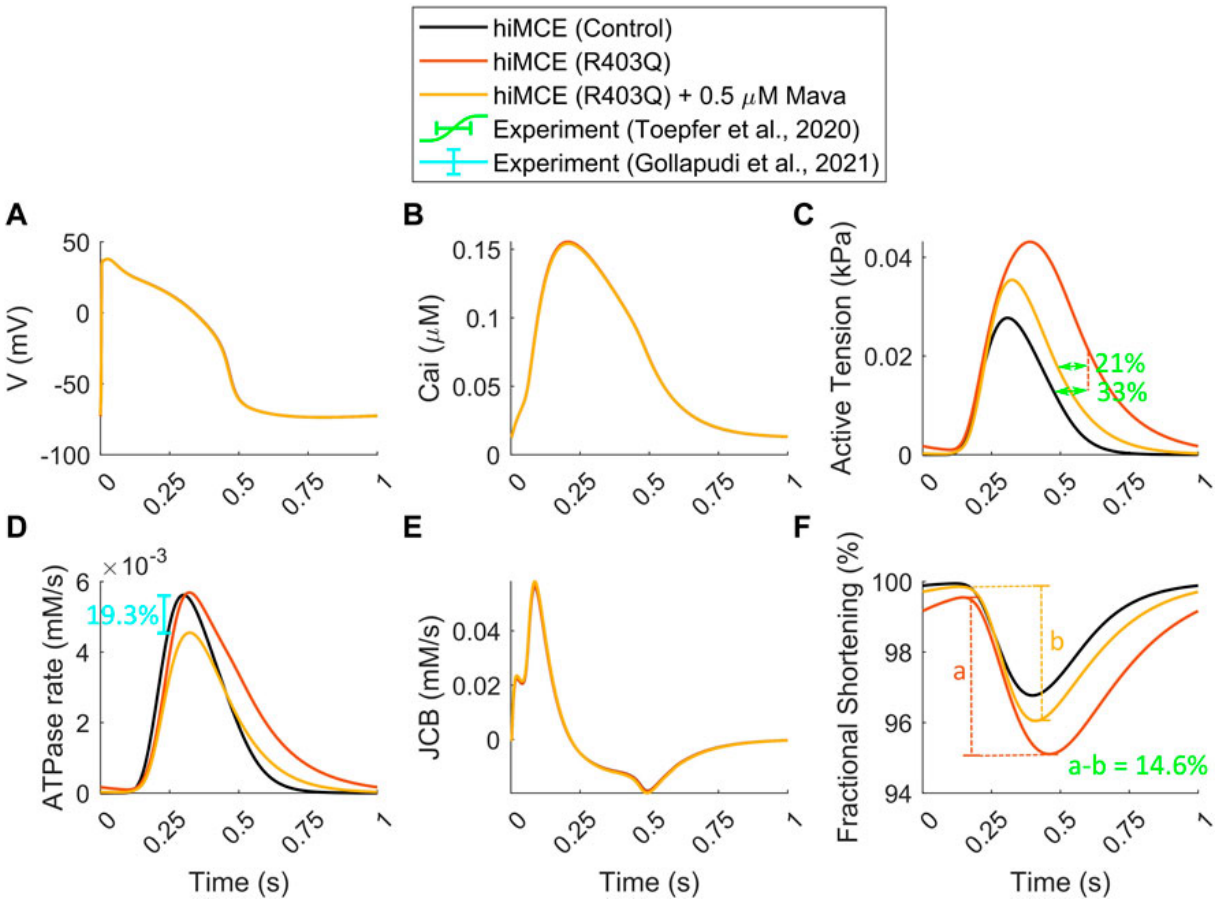

Simulated action potential (A), calcium transients (B), active tensions (C), ATPase rate (D), flux of Ca2+ towards the myofilament (E), and fractional cell shortenings (F) in control and R403Q hypertrophic variant of the in silico model, as well as impact of Mavacamten (Mava, cardiac myosin inhibitor drug). The percents of prolonged tension relaxation in R403Q (C), the reduction in tension relaxation due to MAVA (C), the reduction in fractional shortening in R403Q due to MAVA (F), and the reduction in ATPase rate due to MAVA (D) agree with the experimental data (Toepfer et al., 2020; Gollapudi et al., 2021). (Figure reproduced under Open Access licence from[13]).

Table 4 – Electro-chemo-mechanical biomarkers for calibration of the hiPSC-CM POMs in MYH7(R403Q)

No.	Biomarker	Healthy value (mean ± SD)	Value in MYH7(R403Q) (mean ± SD)
1	APA (mV)	104±6	n/a
2	MDP (mV)	-75.6±6.6	n/a
3	AP CL (ms)	1700±548	n/a
4	dV/dt max (V/s)	27.8±26.3	n/a
5	APD_{10} (ms)	74.1±26.3	n/a

[13] Forouzandehmehr et al. (2022). Altered contractility in mutation-specific hypertrophic cardiomyopathy: A mechano-energetic in silico study with pharmacological insights. Front Physiol 13. doi: 10.3389/fphys.2022.1010786

6	APD_{30} (ms)	180±59	n/a
7	APD_{90} (ms)	415±119	no change
8	AP_{Tri}	2.5±1.1	n/a
9	CT duration (ms)	805±188	no change
10	CT $tRise_{10,\ peak}$ (ms)	270±108	no change
11	CT $tRise_{10,50}$ (ms)	82.9±50.5	no change
12	CT $tRise_{10,90}$ (ms)	167±70	no change
13	CT $tDecay_{90,10}$ (ms)	410±100	no change
14	AT_{amp} (kPa)	0.055±0.009	n/a
15	RT_{50} (ms)	158±12.1	+35.0%
16	%FS	3.27±0.37	+35.8%

APA, AP amplitude; MDP, maximum diastolic potential; CL, cycle length; dV/dtmax, maximum upstroke velocity; APD10-30-90, AP duration at 10, 30 and 90 % of repolarisation; Tri, AP triangulation index; CTduration, calcium transient duration; CT tRise10,peak, time to peak of calcium transient; CTtRise10,50 and CTtRise10,90, rise time from 10 to 50 and 90 % of maximum; CT tDecay90,10, decay time from 90 to 10 % calcium transient amplitude; ATamp, amplitude of active tension; RT50, time from peak contraction to 50% of relaxation; %FS, percentage of fractional shortening.

3.2 Implementation of two new mutated disease variants

3.2.1 MYBPC3 (c.772G>A) in hv-CMs

The MYBPC3:C772G>A is a Tuscany founder mutation causing HCM that affects the cardiac Myosin Binding Protein C (MYBPC3), a thick-filament-associated protein with important structural and functional roles. Pioner *et al.* (2023)[14] reported haploinsufficiency that causes the acceleration of cross bridge kinetics in the sarcomere, and it is responsible for a more energy demanding contraction, together with compensatory/secondary ionic remodelling.

To investigate the effects of the c772G>A variant at the single cell level, we implemented the aspecific/secondary HCM ionic remodelling according to Passini *et al.* (2016)[15] and the mutation specific one according to Pioner, increasing the cross-bridge kinetic rates with a scaling factor between 1.5 and 2.0.

Furthermore, we analysed the model dependency, comparing the effects of the sarcomeric mutation on three different human adult ventricular single cells models considered in this project: the O'Hara-Rudy dynamic[16] (ORd) model, the updated version of ORd by Tomek[17] (ToRORd) and the Bartolucci-Paci-Severi model (BPS). Each electrophysiological model is coupled to the mathematical description of the tension generation according to Land *et al.* (2017). In the BPS-Land model, the maximal active

[14] Pioner et al. (2023). Slower Calcium Handling Balances Faster Cross-Bridge Cycling in Human *MYBPC3* HCM. Circ Res. 132(5):628-644. doi: 10.1161/CIRCRESAHA.122.321956.

[15] Passini et al. (2016). Mechanisms of pro-arrhythmic abnormalities in ventricular repolarisation and anti-arrhythmic therapies in human hypertrophic cardiomyopathy. J Mol Cell Cardiol. 96:72-81. doi: 10.1016/j.yjmcc.2015.09.003.

[16] O'Hara et al. (2011). Simulation of the Undiseased Human Cardiac Ventricular Action Potential: Model Formulation and Experimental Validation. PLoS Comput Biol 7, e1002061. doi: 10.1371/journal.pcbi.1002061

[17] Tomek et al. (2019). Development, calibration, and validation of a novel human ventricular myocyte model in health, disease, and drug block. eLife 8, e48890. doi: 10.7554/eLife.48890

tension at resting length (T_{ref}) has been upscaled of about 30% to adequately reproduce the value of active tension in control conditions.

As a first step, we assessed the effects of the c772G>A variant employing the parameter set from literature (see Figure 8). The simulations show different behaviours among the models, in the generation of active tension (see the third row).

The experimental data on which the HCM remodelling has been formulated includes patch clamp data, mRNA, and protein expression. We performed a semiautomatic parameter tuning selecting a subset of those parameters, specifically the ones related to mRNA and protein expression that only indirectly describe the unpaired electro-mechanical function, and their uncertainty is higher. The results are depicted in Figure 9, and the optimal parameters are collected in Table ***5***. This procedure allowed us to define the mutant baseline parameter set for each model, starting point to characterize the mutant POMs.

Figure 8 – Assessment of model dependency relative to the effects of c772G>A mutation

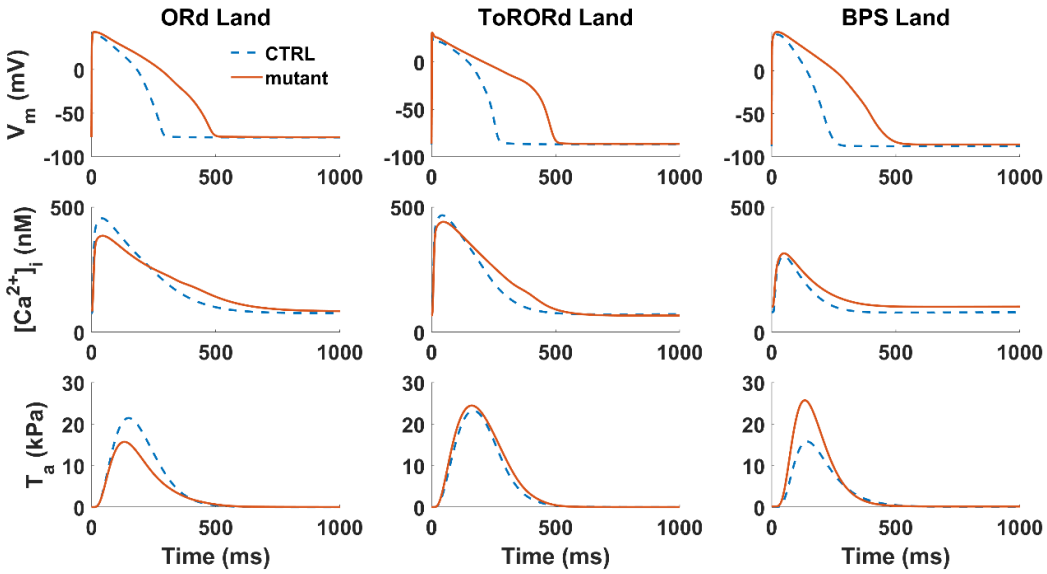

Effects on action potential (first row), calcium transient (second row) and active tension (third row) of the mutation c772G>A on ORd (first column), ToRORd (second column) and BPS (third column) adult ventricular models to evaluate model dependency.

Figure 9 – Effects of the MYBPC3:c772G>A mutation after semiautomatic tuning

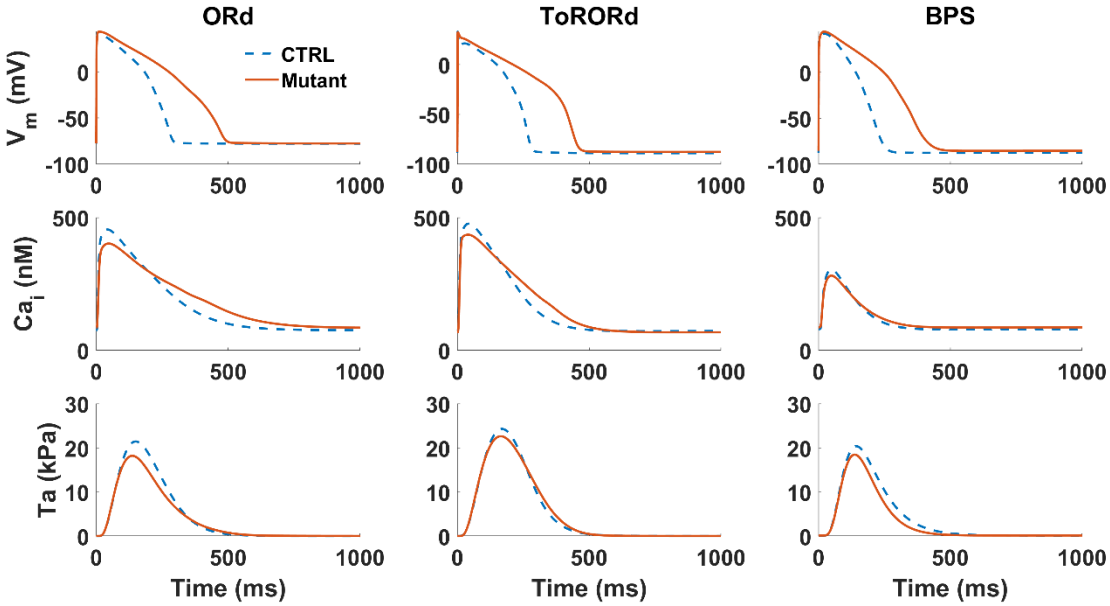

The optimization procedure allows each model to be closer to the experimental data by Pioner et al. (2023)[14]: ΔAPD_{90}% = +70.2%, $\Delta CaTD_{90}$% = +23.9%, ΔCaT_{amp}% = +2.6%, ΔATD_{peak}% = -12.6%, $\Delta ATrt_{50}$% = +0.3%.

Table 5 – Set of parameters underwent to optimisation. Optimal values obtained after the semi-automatic tuning are reported together with the initial guess and the relative percentage change

		ORd Land		ToRORd Land		BPS Land	
Scaling factors	**Initial Guess**	**Par set**	**Δ%**	**Par set**	**Δ%**	**Par set**	**Δ%**
I_{Nab}	2.65	2.87	8.1	2.46	-7.3	2.46	-7.3
I_{Kr}	0.55	0.54	-1.1	0.72	**31.1**	0.70	**26.4**
I_{Ks}	0.55	0.56	1.0	0.48	-12.9	0.63	**15.2**
I_{NaK}	0.70	0.68	-3.2	1.00	**42.3**	0.77	**10.3**
I_{NCX}	1.30	1.25	-4.2	1.26	-3.3	2.30	**+76.9**
J_{up}	0.85	0.82	-3.1	0.86	0.8	1.0	**+17.6**
J_{rel}	0.80	0.88	**10.4**	0.91	**13.7**	0.75	-5.8
k_{off}	0.80	0.83	3.6	0.70	**-12.5**	0.82	3.0
k_{uw}, k_{ws}	2.00	1.96	-1.9	1.61	**-19.6**	1.51	**-24.6**

Following the population approach described above, with the BPS model we obtained 119 calibrated cells on which we applied the MBPC3.c772G>A mutation. 11 cells had to be discarded as stated in methods, remaining with a mutant population of 108 cells, reported in Figure 10.

Figure 10 – MBPC3.c772G>A population results

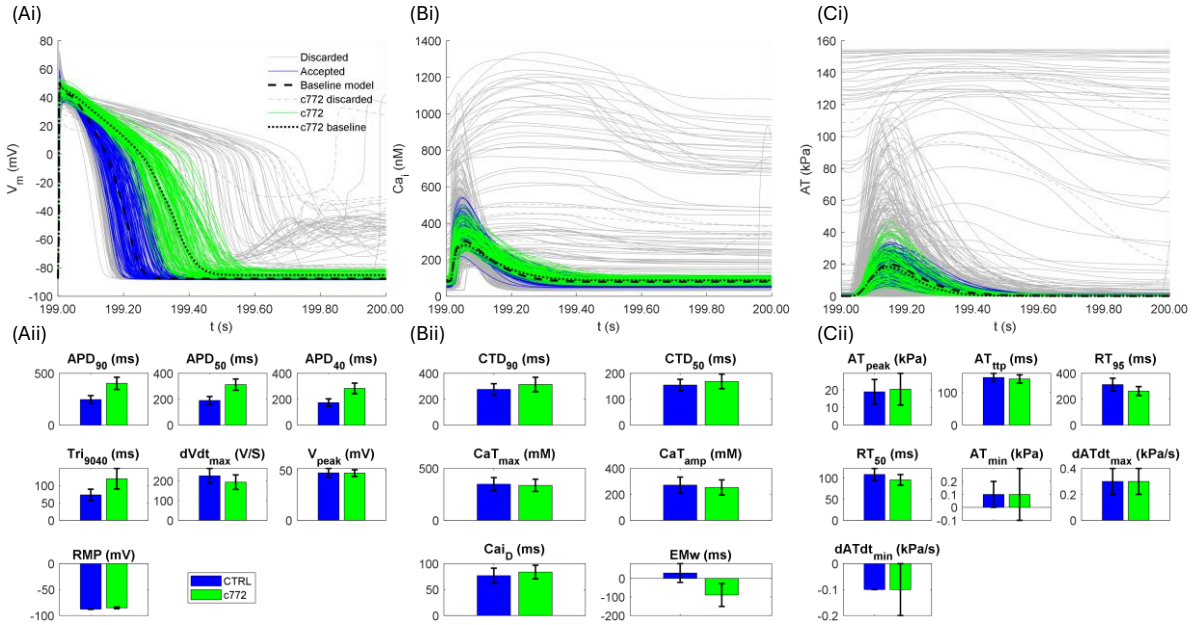

Action potential (A), calcium transient (B) and active tension (C) traces (top) and biomarkers (bottom) of the MBPC3.c772G>A population (green) vs. control (blue).

The analysis of the biomarkers shows an APD prolongation (+63.4%) and an increase in triangulation (APD_{90}-APD_{40}: +63.3%) in the mutant population, while the calcium transient is prolonged to a less extent (+13.8% in $CaTD_{90}$) and relaxation times are shorter (-15.8% in RT_{95}). Peak tension is also similar in the two groups (20.4±9 kPa of the mutation vs. 18.9±7 kPa in control), as found experimentally despite the HCM phenotype[14]. However, the number of induced after-depolarizations grows substantially under the dofetilide protocol: 29 cells show EADs in the mutant population vs 3 in ctrl (2 vs 1 with quinidine). Logistic regression results (Figure 11) show that G_{NaCa}, Ca_{50} and P_{Ca} are the 3 parameters whose increase drives EAD occurrence most, while G_{NaK}, G_{Kr} and $J_{up,max}$ are the 3 most protective ones. This analysis could guide pharmacological interventions to reduce the increased arrhythmic risk of the *MBPC3.c772G>A* mutation, pointing to a reduction in the sodium-calcium exchanger or L-type calcium currents, a sensitization of troponin to Ca^{2+} (lowering Ca_{50}). On the opposite, based on this results one could act on enhancing the sodium-potassium pump or rapid-delayed rectifier currents as, well as on increasing of the SERCA uptake rate.

Figure 11 – MBPC3.c772G>A population logistic regression results

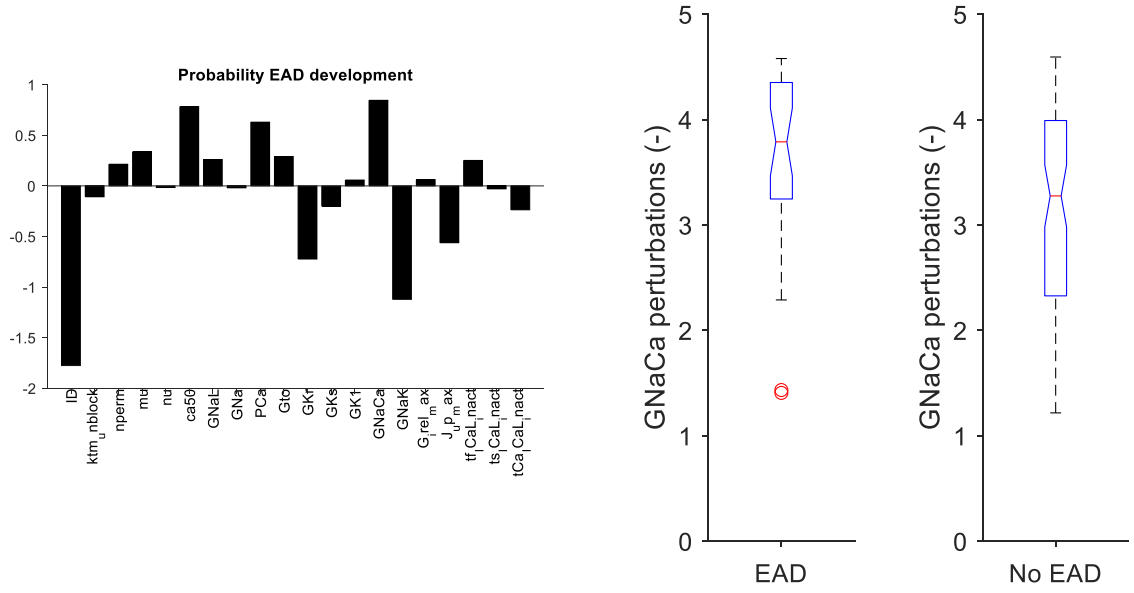

Coefficients of the logistic regression of the dofetilide protocol (left) and statistics of G_{NaCa} values between cells showing EADs vs. cell not showing EADs (right).

3.2.2 JPH2 (T161K) in hiPSC-CMs

Junctophilin-2 (JPH2) is an intracellular protein that supports the so-called junctional membrane complex (JMC) integrity near T-tubules (Figure 12). Specifically, JPH2 ensures the physical proximity of the plasma membrane (and ion channels in it) and sarcoplasmic reticulum (SR). This is essential for an efficient and synchronous excitation–contraction coupling process (i.e., how the electrical activity of the heart is linked to the contractile function at the cell-level).

While HCM is primarily caused by mutations in sarcomeric genes, 5–10% of adults and 25% of children diagnosed with HCM have mutations in the genes that encode non-sarcomeric proteins. JPH2 is one such protein.

Figure 12 – Localisation and role of JPH2 in cardiomyocytes

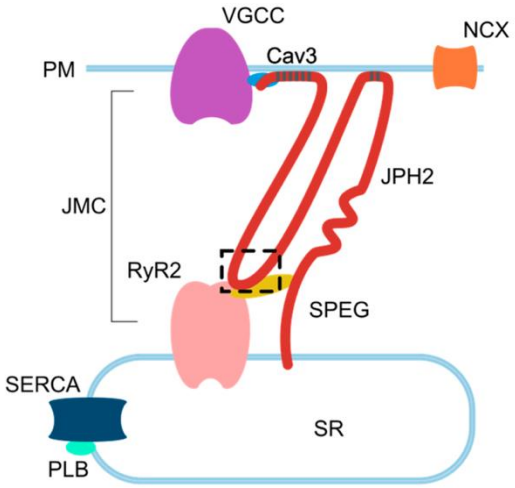

SR, Sarcoplasmic Reticulum; PLB, Phospholamban; SERCA, Sarco/Endoplasmic Reticulum Ca2+-ATPase; SPEG, Striated Muscle Enriched Protein Kinase; RyR2, Ryanodine Receptor 2; JMC, Junctional Membrane Complex;

JPH2, Junctophilin-2; PM, Plasma Membrane; VGCC, Voltage-Gated Calcium Channel; Cav3, Caveolin-3; NCX, Sodium–Calcium Exchanger. (Figure reproduced under Open Access licence from[18]).

A previously published study at TAU investigated the phenotype of a Finnish founder mutation, JPH2 p.(Thr161Lys) or T161K in the short form, hiPSC-CMs *in vitro*[18]. Valtonen *et al.* (2023) showed that mutation-carrying hiPSC-CMs (T161K) exhibit altered calcium ion current dynamics in comparison to the healthy (isogenic) cell line (Figure 13). Specifically, the current decay – fitted with a single exponential – was measured to have a 1.54-fold larger time constant (Figure 13G).

Figure 13 – Calcium current (ICa) in T161K and isogenic hiPSC-CMs

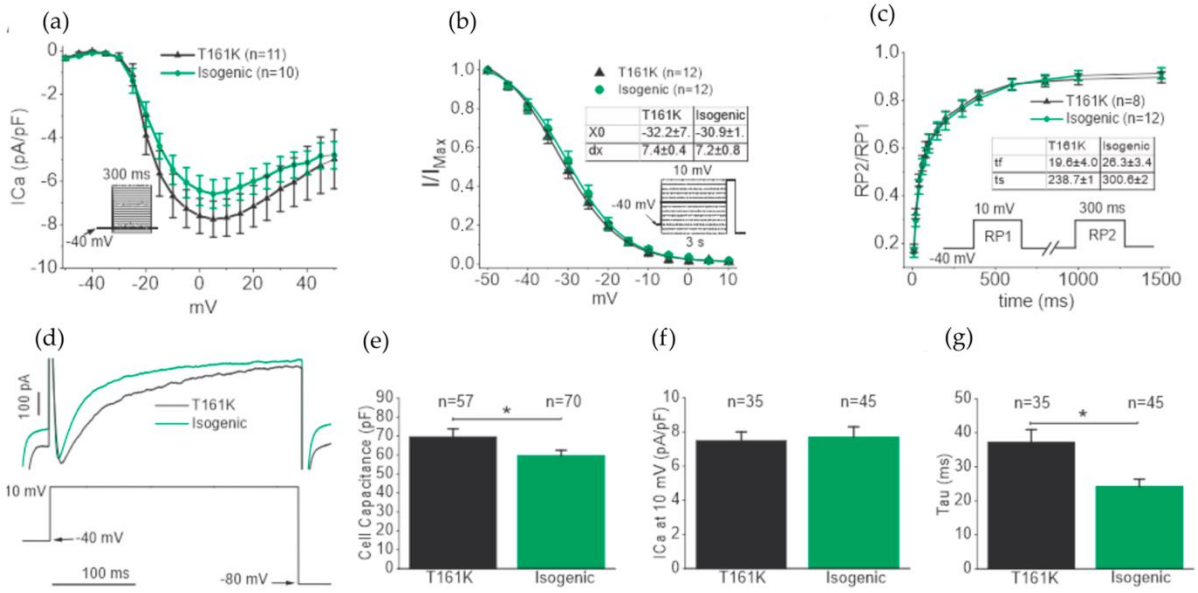

(a) Current density–voltage relationship of ICa recorded from T161K and isogenic hiPSC-CMs. (b) Voltage-dependent inactivation curve of ICas. (c) Average time course of recovery from inactivation of ICa. Peak calcium currents elicited by P2 were normalized (I2/I1) and plotted as a function of the recovery interval. (d) ICa responses to step voltage protocol. (e) Comparison of cell capacitances (p < 0.05, unpaired t-test). (f) Comparison of ICa current densities at 10 mV. (g) Comparison of decay time constant of ICa obtained from monoexponential fitting. (Figure reproduced under Open Access licence from[18]).*

We implemented a JPH2 (T161K) variant of our hiPSC-CM model[13], based on the Valtonen *et al.* (2023) *in vitro* data by multiplying the time constants of L-type calcium current inactivation with a factor of 1.54 (see Table 1 for further explanation of the parameters). Comparison of the action potential (AP) morphology as a principal output shows that our *in silico* model variant replicates the *in vitro* phenotypes rather accurately (Figure 14).

[18] Valtonen, Prajapati et al. (2023). The Junctophilin-2 Mutation p.(Thr161Lys) Is Associated with Hypertrophic Cardiomyopathy Using Patient-Specific iPS Cardiomyocytes and Demonstrates Prolonged Action Potential and Increased Arrhythmogenicity. Biomedicines 11 #1558, 1–19. doi: https://doi.org/10.3390/ biomedicines11061558

Figure 14 – Action potential properties in T161K and isogenic hiPSC-CMs

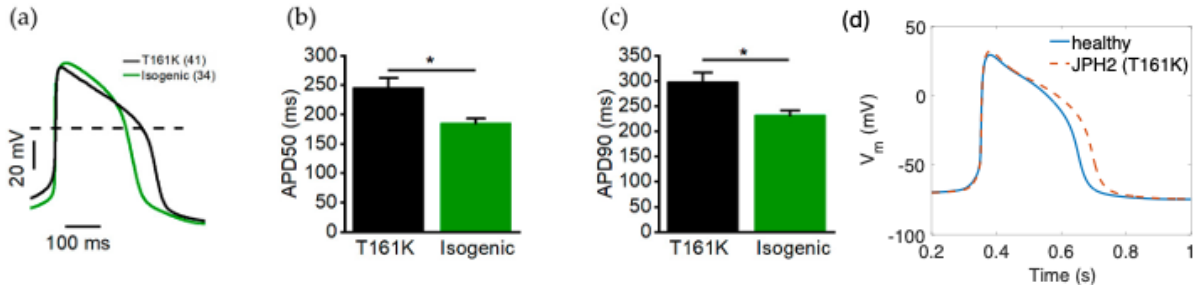

(a) Representative spontaneous AP traces from T161K hiPSC-CMs and isogenic hiPSC-CMs. (b,c) Averaged values for AP duration at 50% (APD50) and 90% (APD90) repolarisation. (d) Simulated AP in the healthy and mutated hiPSC-CM model variants in silico (Panels A-C reproduced under Open Access licence from[18]).

Table 6 – Electro-chemo-mechanical biomarkers for calibration of the hiPSC-CM POMs in JPH2

No.	Biomarker	Healthy value (mean ± SD)	Value in JPH2 (mean ± SD)
1	APA (mV)	104±6	n/a
2	MDP (mV)	-75.6±6.6	n/a
3	AP CL (ms)	1700±548	n/a
4	dV/dt max (V/s)	27.8±26.3	no change
5	APD_{10} (ms)	74.1±26.3	n/a
6	APD_{30} (ms)	180±59	n/a
7	APD_{90} (ms)	415±119	+35.9%
8	AP Tri	2.5±1.1	n/a
9	CT duration (ms)	805±188	n/a
10	CT $tRise_{10,\ peak}$ (ms)	270±108	n/a
11	CT $tRise_{10,50}$ (ms)	82.9±50.5	n/a
12	CT $tRise_{10,90}$ (ms)	167±70	n/a
13	CT $tDecay_{90,10}$ (ms)	410±100	n/a
14	AT magnitude (kPa)	0.055±0.009	n/a
15	RT_{50} (ms)	158±12.1	n/a
16	%FS	3.27±0.37	**n/a**

Please, see Table 4 for the descriptions of the biomarkers.

Employing **approach III** (Figure 3), we used three baseline models derived from the Forouzandehmehr *et al.* (2024)[11] hiPSC-CM model (Healthy, JPH2, and MYH7) to create the populations. Each baseline model was extended into a candidate population of 10 000 virtual cells by adjusting parameters described in Table 1 to range [50, 200] %. Then, the three populations were cross-calibrated using the healthy and JPH2 biomarker sets (Table 6) and MYH7 biomarker set (Table 4). This was done to illustrate, how the number of cross-calibrated models (Table 7) is impacted by applying less or more constricting biomarker sets to the uncalibrated POMs. That is, the healthy biomarker set is extensive, while the JPH2 set is very scarce.

Table 7 – Populations of hiPSC-CM models using different biomarker sets in cross-calibration

	The uncalibrated POMs that are cross-calibrated		
Biomarker set applied to the uncalibrated POMs	Healthy	JPH2	MYH7
JPH2	2950	2304	2779
MYH7	5	3	32
Healthy	2	1	8

The POMs analysis indicated a problem with the hiPSC-CM model that needs to be addressed in the upcoming work: the contractile element is overly sensitive to changes in parameter values. Thus, when complete set of contractile biomarkers, which are included in the healthy biomarker set, are used to calibrate the candidate population, hardly any of the virtual cells pass the calibration.

3.2.3 JPH2 (T161K) in hv-CMs

As a first approach, the same changes found in hiPSC-CM were applied to the control hv-CM population consisting in 119 adult ventricular cells, as reported above. After removing the cells showing repolarisation failure or unphysiological ion concentrations due to the mutation, the JPH2 (T161K) population consisted in 88 hv-CMs, reported in Figure 15.

Figure 15 – JPH2 (T161K) population results

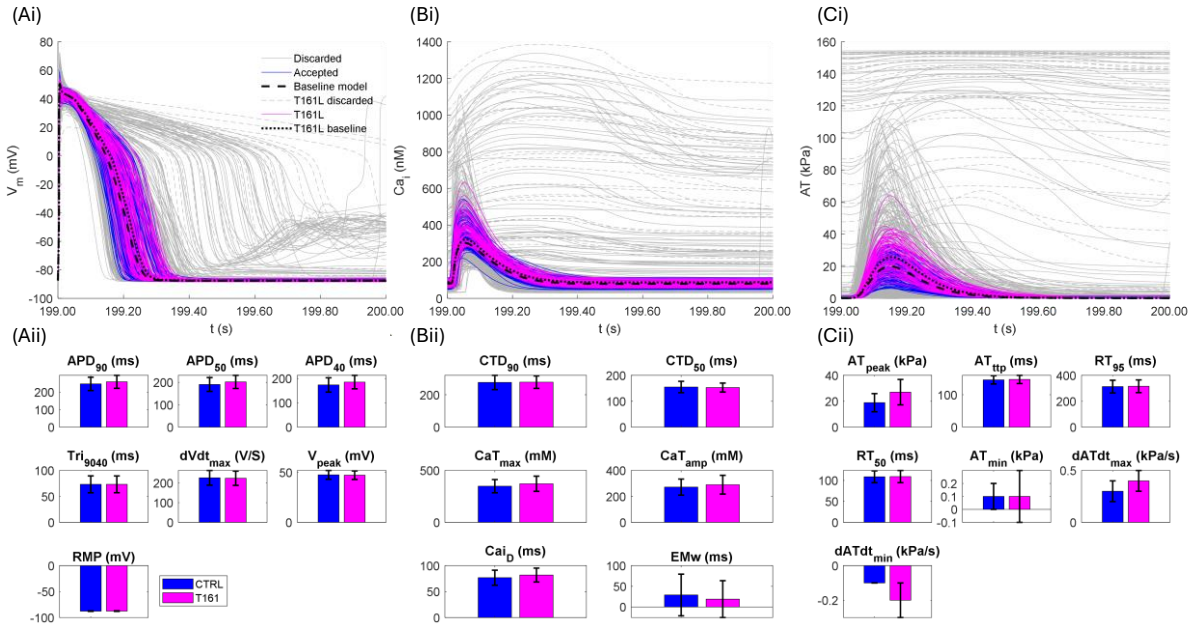

Action potential (A), calcium transient (B) and active tension (C) traces (top) and biomarkers (bottom) of the JPH2 (T161) population (magenta) vs. control (blue).

Despite the small APD prolongation (+4.8% in APD_{90}), compared to experimental data on hiPSC-CMs, peak active tension is increased on average (+42.9%), and the population shows a slightly increased arrhythmogenicity: 3 and 9 cells show EADs with the quinidine and dofetilide protocol, respectively (vs. 1 and 3 in control).

4 Conclusions and outlook

Summary of implemented simulation tools and disease model variants:

- We have developed an open-source POMs framework that is freely available for download and further use on GitHub.
- We have demonstrated that the tool has the required functionality (like the previous in-house, research-oriented software tools), while having broader functionality, better scalability, and user-friendly design.
- We have established a library of five HCM-related mutation-specific model variants and extended it to POMs, including the previously published work and two newly implemented HCM mutations.
- According to the simulation we ran, the inclusion of the HCM remodelling is responsible for an increase of proarrhythmicity.

The presented ***Deliverable 4.1 Libraries of HCM populations of cellular electromechanical models*** functions as a base for the work focusing on tissue and patient scale modelling and simulations in WP4. Specifically, ***D4.1*** findings and solutions will feed into task leading to ***D4.2 Technologies for optimal therapy choice***.

The established modelling frameworks and implemented simulation software tools will be exploited in the work ahead in WP4, to

- add further mutation variants of the hiPSC- and hv-CM models, based on newly available *in vitro* characterisations;
- derive features of cellular pro-arrhythmic factors to be used as complementing data in WP6;
- stratify disease markers of arrhythmogenicity, impaired conduction and mechanical dysfunction;
- explore and predict safety and efficacy of candidate drug molecules, across HCM variants.